Green Synthesis of Reduced $Ti_3C_2T_x$ MXene Nanosheets with Enhanced Conductivity, Oxidation Stability, and SERS Activity

Tej B. Limbu,[†] Basant Chitara,[†] Jason D. Orlando,[†] Martha Garcia Cervantes,[†] Shalini Kumari,[‖] Qi Li,[‖] Yongan Tang,[‡] Fei Yan,[†]*

[†]Department of Chemistry and Biochemistry, North Carolina Central University, Durham, NC 27707, USA

[‡]Department of Mathematics and Physics, North Carolina Central University, Durham, NC 27707, USA

[‖]Department of Physics, The Pennsylvania State University, University Park, PA 16802, USA
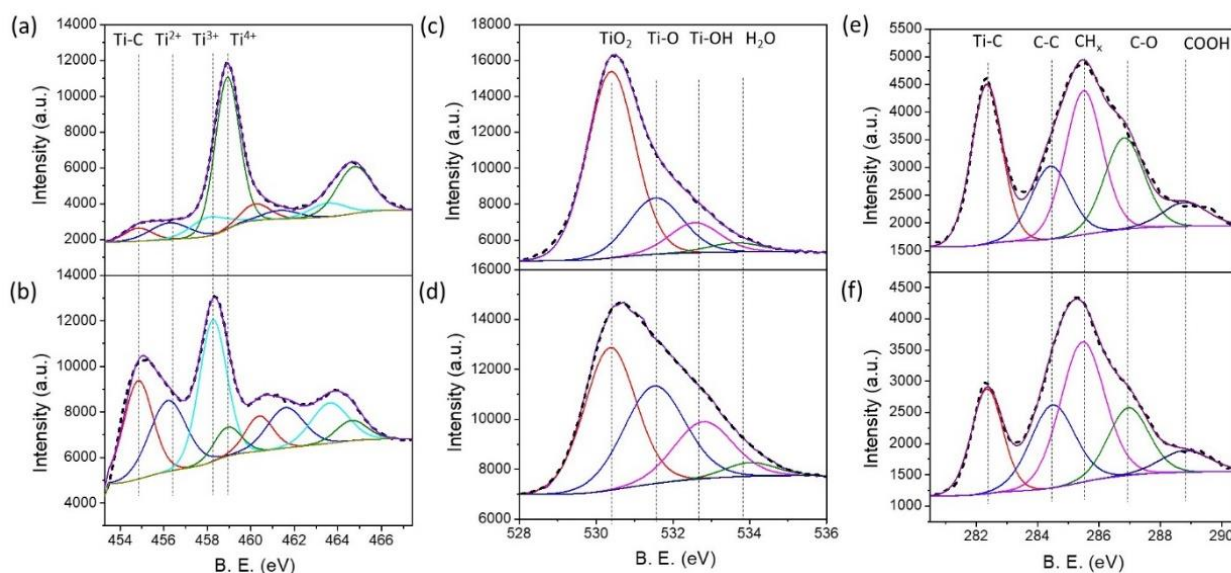
Deconvolution of XPS fine peaks for Ti2p, O1s, and C1s

Figure S1. Deconvolution of Ti2p peak for (a) $Ti_3C_2T_x$, (b) r-$Ti_3C_2T_x$, O1s peak for (c) $Ti_3C_2T_x$, (d) r-$Ti_3C_2T_x$, and C1s peak for (d) $Ti_3C_2T_x$, € r-$Ti_3C_2T_x$

Details of electrical measurements

The metal contact pads on MXene films (Figure S2a and S2b) were deposited using a shadow mask in electron-beam evaporation. The thickness of Ti and Au in the pads are 20 and 300 nm, respectively. Our shadow mask consists of rectangular holes of dimension, 200x300 µm, separated with different pitches, 30, 50, 60, 100, 200 and 300 µm. After the deposition of the contact pads, SEM images were taken, and the separation of the contact pads was measured using a software, Image J. The averaged measured values of the six different contact spacings are 24, 43, 53, 93, 192, and 293 µm. Figure S2c and S2d show high magnification SEM images of the $Ti_3C_2T_x$, and r-$Ti_3C_2T_x$ films.
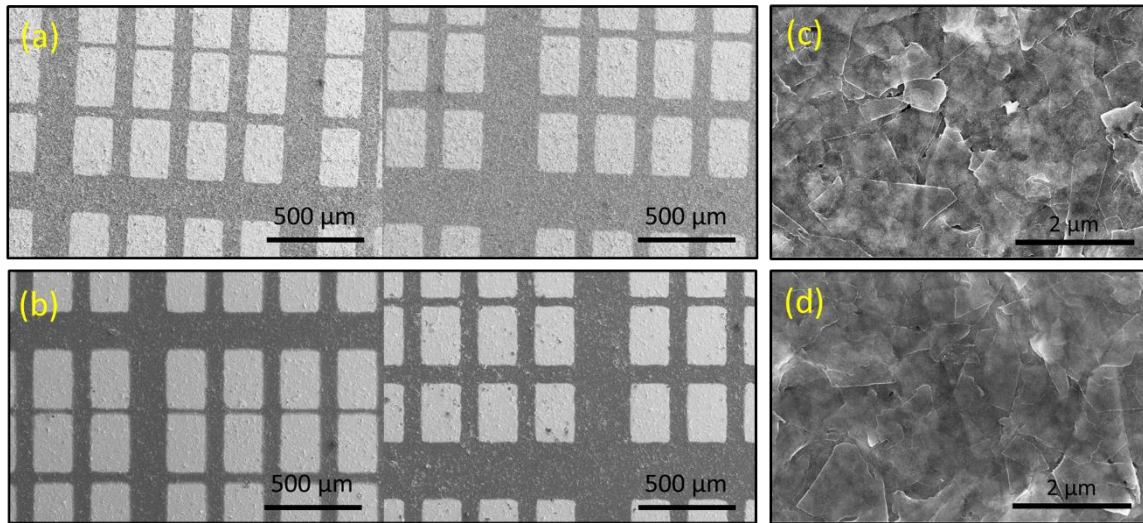
Figure S2. SEM images of 20 nm-Ti/300 nm-Au contact pads on (a) $Ti_3C_2T_x$, and (b) r-$Ti_3C_2T_x$ films on SiO_2/Si, and high magnification images of (c) $Ti_3C_2T_x$, and (b) r-$Ti_3C_2T_x$ films.

Calculation of Electrical conductivity and contact resistivity

The total resistance of the MXene films can be expressed as:

$$R_T = R_{MXene} + 2R_c + 2R_p \qquad (1)$$

, where R_{MXene} is the resistance offered by MXene films, R_c is the contact resistance associated with the metal pad-MXene film interface, and R_p is the resistance at the metal pad-probe contact. The measurements were carried out with two probes. As expected, we found that total resistance values measured at various contact pad spacings; 24, 43, 53, 93, 192, and 293 μm, following a linear increase with pad spacings (see Figure 4b and 4c), and the measured total resistance ranges between 8.4 to 10.3 $K\Omega$ for Ti$_3$C$_2$T$_x$ and 1.1 to 1.4 $K\Omega$ for r-Ti$_3$C$_2$T$_x$ films. Neglecting the small value of $R_p(\sim 12\ \Omega)$ measured in our case, we are left with the following relation:

$$R_T = R_{MXene} + 2R_c \tag{2}$$

Finally, plugging in the equation 2 the value of $R_{MXene} = R_s(L/W)$, we obtain the following equation:

$$R_T = (R_s/W)L + 2R_c \tag{3}$$

, where L and W are spacing and width of the contact pads, respectively. Slopes of the fitted lines in Figures 4b and 4c are 6.87 and 1.39, respectively. The sheet resistance values are calculated with the relation:

$$R_s = Slope\ x\ W \tag{4}$$

we obtained sheet resistance values as 1415 ± 125 and 288 ± 27 Ω/sq for Ti$_3$C$_2$T$_x$ and r-Ti$_3$C$_2$T$_x$, respectively. With the measured thicknesses as 1.5 and 1.2 μm for Ti$_3$C$_2$T$_x$ and r-Ti$_3$C$_2$T$_x$ films, the corresponding conductivity values are calculated using the relation:

$$Conductivity = 1/(R_s\ x\ Thickness) \tag{5}$$

471 ± 49 and 2819 ± 306 S/m, respectively. We also obtained the contact resistance of Ti/Au pad with MXene films from the y-intercept values in Fgures 4a and 4b, which are 4.2 ± 0.4 and 0.5 ± 0.05 $K\Omega$ for Ti$_3$C$_2$T$_x$ and r-Ti$_3$C$_2$T$_x$ films, respectively. Each metal contact pad has the area:

A= 206 x 307 μm^2 = 6.3×10^{-8} m^2

Hence, the contact resistivities are measured to be $(2.6 \pm 0.3) x 10^{-4}$ and $(3.3 \pm 0.4) x 10^{-5}$ Ωm^2 for Ti$_3$C$_2$T$_x$ and r-Ti$_3$C$_2$T$_x$ films, respectively.

Thickness Measurement for Ti$_3$C$_2$T$_x$ and r-Ti$_3$C$_2$T$_x$ films
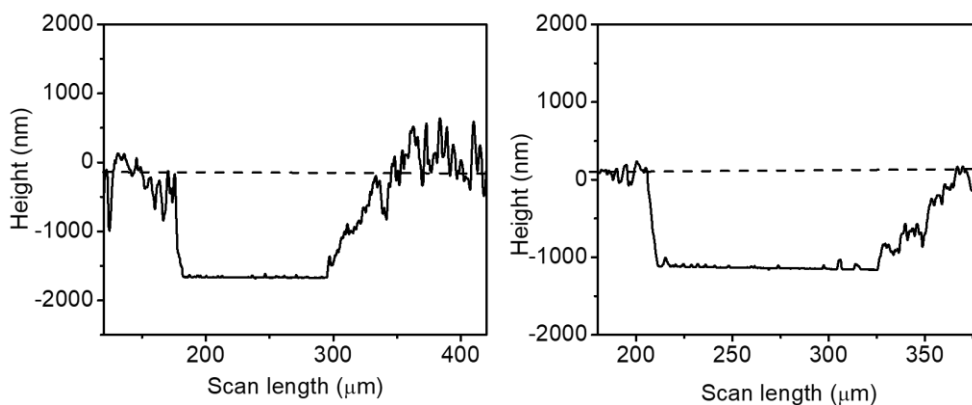
Figure S3. Height profile of (a) Ti$_3$C$_2$T$_x$, and (b) r- Ti$_3$C$_2$T$_x$ films on SiO$_2$/Si. The steps were created by scrapping out a small portion of the films with a blade.
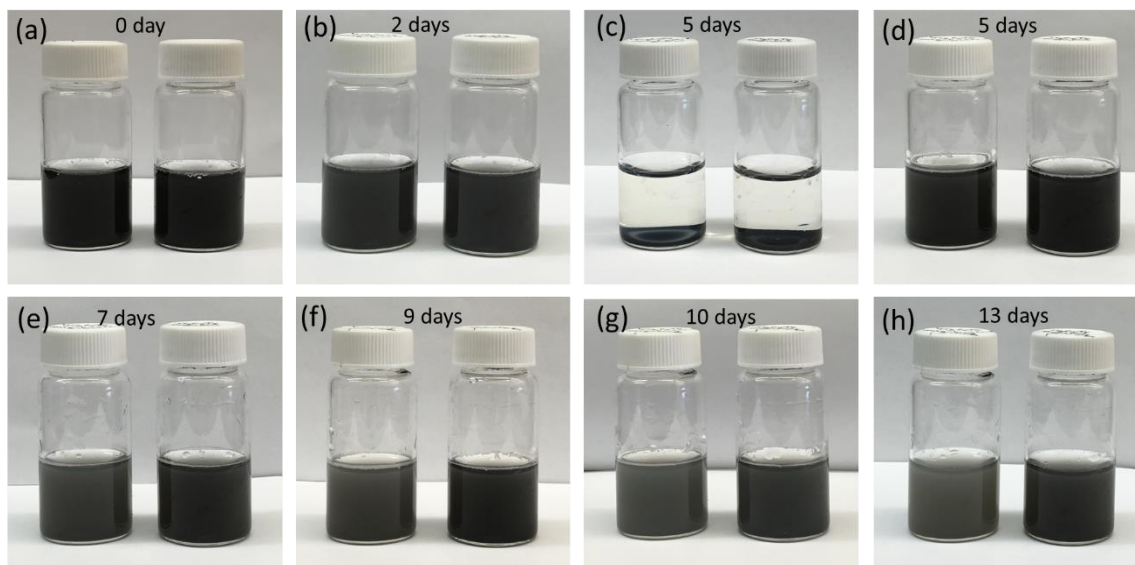
MXene oxidation stability test

Figure S4. Photographs of Ti$_3$C$_2$T$_x$ (left) and r-Ti$_3$C$_2$T$_x$ (right) with a lower concentration, 5 mg in 10 ml of water: Freshly prepared (a), after 2 days (b), after 5 days before shaking (c), after 5 days (d), after 7 days (e), after 9 days (f), after 10 days (g), and after 13 days (h)

SEM analysis of degraded $Ti_3C_2T_x$ and r-$Ti_3C_2T_x$

It is evident from the SEM images that TiO_2 nanoparticles grow on MXene basal planes and their size and density continue to increase with time. After 3 days of exposure to water, $Ti_3C_2T_x$ basal planes are densely covered with the nanoparticles. However, the TiO_2 nanoparticles are small and sparse on the r-$Ti_3C_2T_x$ basal planes compared to $Ti_3C_2T_x$. After 14 days, the size and density of the TiO_2 nanoparticles grow in both of the samples, but they are smaller and less dense on r-$Ti_3C_2T_x$ than on $Ti_3C_2T_x$. After 21 days, basal planes of both Ti3C2Tx and r-$Ti_3C_2T_x$ are covered completely with TiO_2 nanoparticles. However, TiO_2 nanoparticle size and thickness of the oxide layer is bigger on $Ti_3C_2T_x$ than on r-$Ti_3C_2T_x$.
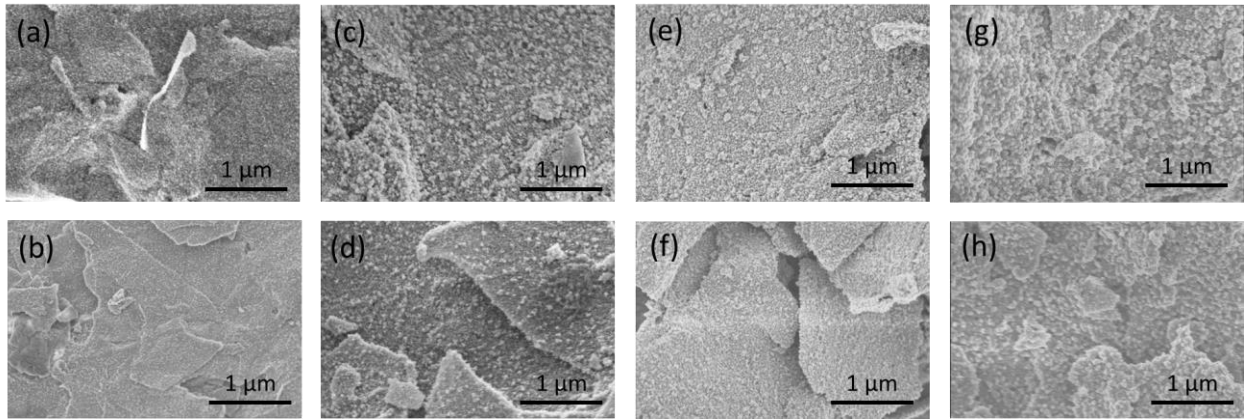
Figure S5. SEM micrographs of $Ti_3C_2T_x$ (upper) and r-$Ti_3C_2T_x$ (lower) after allowing to degrade in water for (a, b) 3 days, (c, d) 14 days, (e, f) 21 days, and (g, h) 28 days)

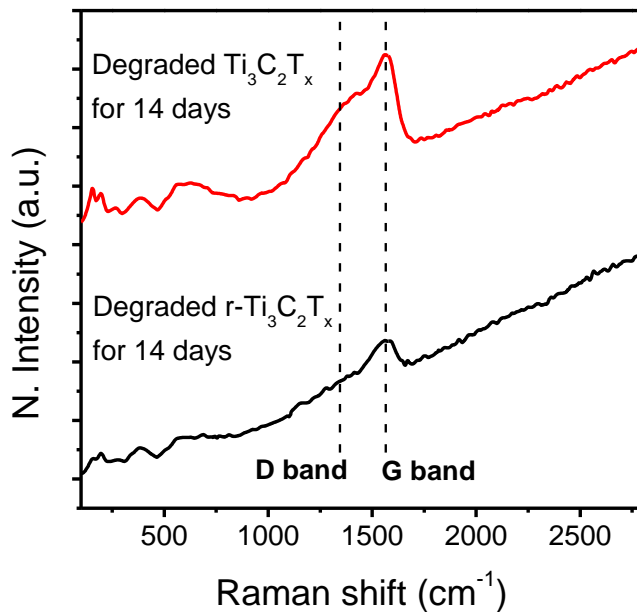**Raman spectra of disordered carbon material formed on MXene**

Figure S6. Raman spectra of Ti₃C₂Tₓ (red) and r-Ti₃C₂Tₓ exposed to water for 14 days. Disordered carbon material forms as indicated by D and G bands in the spectra.

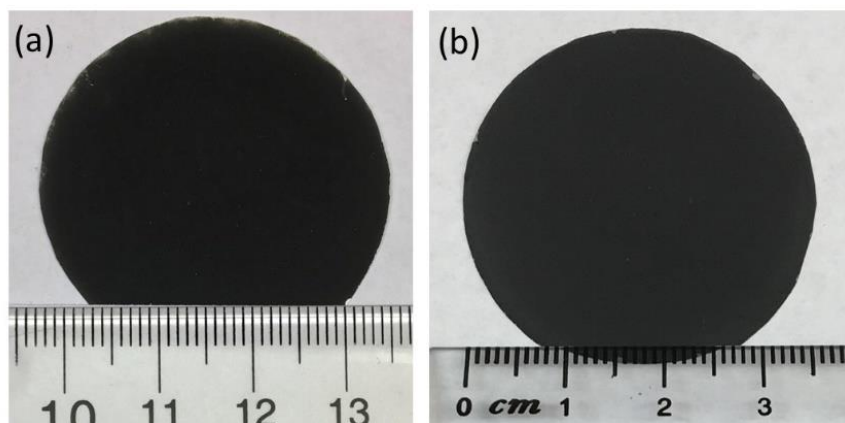**Photographs of the SERS substrates on PVDF filter membranes**

Figure S7. Photographs of the SERS substrates prepared with (a) Ti₃C₂Tₓ and (b) r-Ti₃C₂Tₓ on PVDF filter membrane

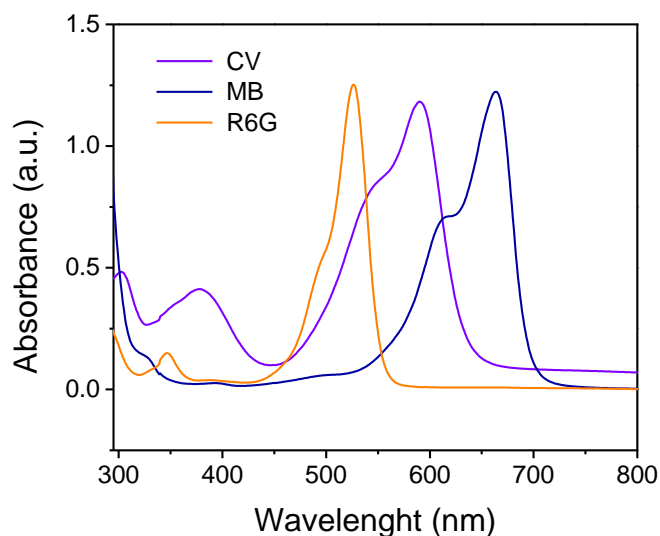**UV-vis absorption spectra of CV, MB, and R6B**

Figure S8. UV-vis absorption spectra of CV, MB, and R6B showing absorption peaks at different wavelengths; 527, 591, and 663 nm, respectively.

Examination of plasmonic absorption in Ti$_3$C$_2$T$_x$ and r-Ti$_3$C$_2$T$_x$
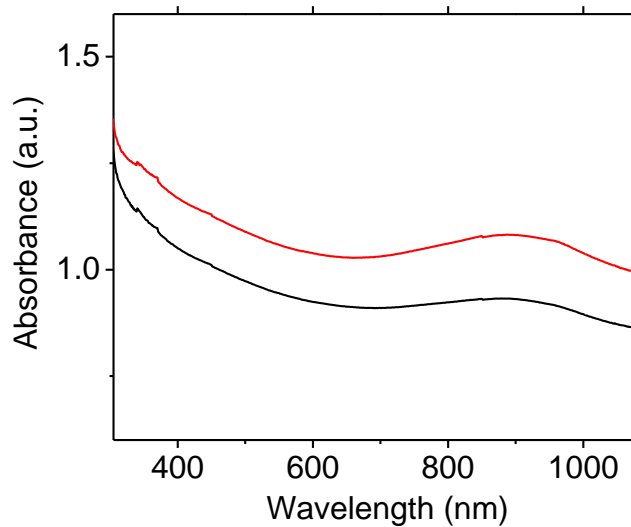
Figure S9. UV-vis absorption spectra of Ti$_3$C$_2$T$_x$ and r-Ti$_3$C$_2$T$_x$